

Design and experimental study of the end-effector for broccoli harvesting

Xiong Zhao^{1,2}, Gangji Xu¹, Pengfei Zhang³, Gaohong Yu^{1,2}, Yadan Xu^{3*}

(1. Faculty of Mechanical Engineering, Zhejiang Sci-Tech University, Hangzhou 310018, China;

2. Key Laboratory of Transplanting Equipment and Technology of Zhejiang Province, Hangzhou 310018, China;

3. Hangzhou Vocational & Technical College, Hangzhou 310018, China)

Abstract: The end-effector is an important part of the broccoli harvesting robot. Aiming at the physical characteristics of a large broccoli head and thick stem, a spherical cutting tool broccoli harvesting end-effector was designed in this study. First, the physical characteristics of broccoli were tested, and physical parameters such as the broccoli head diameter and stem diameter of broccoli were measured. The maximum cutting force of broccoli stems under different cutting angles was tested. Second, according to the physical characteristics and harvesting process of broccoli, the end-effector was designed, and the mathematical model of kinematics and dynamics was established. Based on the results of dynamic analysis, the end-effector rod was optimized, and the unilateral width of the slider was 40 mm, the length of the connecting rod was 120 mm, and the length of the crank was 42 mm. The mechanism needed an external driving force of 140.54 N to cut the broccoli stem. Therefore, a 32 mm cylinder with a load rate of 50% was selected as the power source. Finally, the feasibility of the broccoli harvesting end-effector was verified by the harvesting test. Experiments showed that the overall harvesting success rate of the end-effector is 93.3%, and the smoothness rate of the stem section is 83.3%. The harvesting performance of the broccoli end-effector was verified. This lays a foundation for agricultural robots to harvest broccoli.

Keywords: harvesting robot, broccoli, end-effector, dynamic analysis, mechanism optimization

DOI: [10.25165/j.ijabe.20241701.8110](https://doi.org/10.25165/j.ijabe.20241701.8110)

Citation: Zhao X, Xu G J, Zhang P F, Yu G H, Xu Y D. Design and experimental study of the end-effector for broccoli harvesting. *Int J Agric & Biol Eng*, 2024; 17(1): 137–144.

1 Introduction

China is a large country of broccoli planting. The total planting area of broccoli and cauliflower is approximately 561 000 hm², and the yield reaches 10.936 Mt^[1]. The production process is usually dominated by manual harvesting^[2,3], which has the disadvantages of low efficiency, high labour intensity and high cost^[4,5]. The development of agricultural harvesting robots provides a material basis for improving production efficiency, changing the mode of development and enhancing the comprehensive agricultural production capacity^[6-9]. As an important part of agricultural harvesting robots, the harvesting performance of harvesting end-effectors has an important influence on the overall efficiency and performance of harvesting robots^[10-12]. Therefore, the development and design of an end-effector is of great significance to broccoli harvesting robots.

In recent years, domestic and foreign scholars have studied the growth environment and fruit characteristics of different crops and designed special harvesting actuators for the harvesting of round fruits such as apple^[13,14], citrus^[15,16], and tomato^[17,18] and 'strip' fruits such as cucumber^[19,20] and green pepper^[21,22]. According to the different harvesting methods, the end-effector can be categorized

into the force detachment type and cutting detachment type. The force detachment type harvests by grasping the fruit and twisting the stem. The end-effector generally adopts suction cup type, multifinger type and other mechanisms. For example, Wei et al.^[16] proposed an underactuated citrus picking end-effector using a three-finger structure to wrap the surface of the citrus and twist it for harvesting. Guo et al.^[17] proposed a bionic underactuated flexible claw tomato end-harvesting end-effector based on the bionic principle of the FRE structure and finger design. The bionic principle makes the end finger more suitable for the outer surface of the tomato. The surface coverage of tomato reached 23.6%-32.5%. The cutting-off type is achieved by wrapping the fruitage and using the cutting tool to cut the stem to achieve harvesting. Li et al.^[12] proposed a fruit-closing apple picking end-effector, and the blade and the tooth-shaped fruit-closing device were used to cut the stem to achieve harvesting. Wang et al.^[15] proposed a bite-type end-effector for citrus picking by simulating snake beak swallowing, which realized citrus picking at different stem angles. There are few studies on vegetable harvesting end-effectors for broccoli at home and abroad. The head of broccoli is huge, the stem is thick, and it is not suitable for harvesting in a force detachment type. The general cutting-off end-effector is not suitable for harvesting large ground vegetables such as broccoli, but it provides some ideas for research.

Aiming at the physical characteristics of large fruits and stout stems of broccoli, this paper designs and develops a shear-detached broccoli harvesting end-effector. The end-effector adopts a four-bar mechanism as the configuration, and the spherical cutting tool is used as the harvesting cutting tool. According to the physical characteristics test results of the broccoli stem, the genetic algorithm rod length is optimized by dynamic analysis under the condition of minimum end driving force.

Received date: 2022-12-22 **Accepted date:** 2023-12-28

Biographies: Xiong Zhao, Professor, research interest: mechanism design, non-circular gear transmissions, and agricultural machinery, Email: zhaoxiong@zstu.edu.cn; Gangji Xu, Master candidate, research interest: agricultural machinery, Email: 1210594542@qq.com; Pengfei Zhang, Lecturer, research interest: agricultural machinery, Email: 527677162@qq.com; Gaohong Yu, Professor, research interest: machine design, non-circular gear transmissions and control, agricultural machinery, Email: yugh@zstu.edu.cn.

*Corresponding author: Yadan Xu, Associate Professor, research interest: agricultural machinery. Hangzhou vocational & Technical College, Hangzhou 310018, China. Tel: +86-13456820528, Email: xuyadan2005@163.com.

2 Physical characteristics test of broccoli

2.1 Mechanical characteristics test materials and equipment

2.1.1 Testing material

In this study, 'ZheQing 161' broccoli was selected as the research object. After picking, it was preserved and transported to the laboratory for testing. To ensure the freshness of broccoli, the diameter of broccoli head D , height of broccoli head H , diameter of stem d , and weight of broccoli head W were measured, and the mechanical properties of stem were tested. Broccoli includes broccoli buds, lateral leaves, and stems. The mature broccoli is shown in Figure 1. The broccoli cutting figure is shown in Figure 2. The stem can be divided into two parts: the external cortex and internal tissue. The external cortex contains mechanical structures such as the epidermis and phloem, with high cellulose content and thick cell walls, so it has strong toughness and high hardness. The internal tissue contains medullary tissue, the cell wall is thin, the internal water is sufficient, the overall toughness is poor, and the brittleness is high.



Figure 1 Mature field broccoli

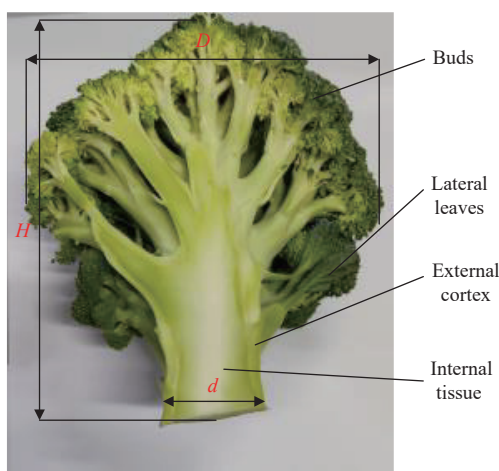
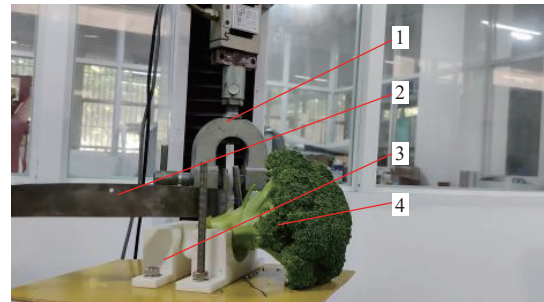


Figure 2 Broccoli cutting figure

2.1.2 Testing equipment

In this experiment, the diameter D , height H , stem diameter d and weight W of broccoli heads were measured by a precision 'π' ruler (range 100-225 mm), steel ruler (range 30 cm), Vernier calliper and electronic scale (range 1 kg). The mechanical properties of broccoli stems were tested on the test bench shown in Figure 3, which included a microcomputer-controlled electronic universal material testing machine (Model: LDW-1; Maximum load: 50 kg;

Power: 12 kW; Manufacturer: Shanghai Songton Machinery Equipment Co., Ltd., China), spherical cutting tool (blade angle of 30°, outer diameter of 160 mm, blade thickness of 4 mm) and cutting platform. The stem of broccoli is strong and has a certain degree of lignification. Therefore, the blade angle of the tool is 30°. The spherical cutting tool and cutting platform were fixed and installed on the test bench through the test bench fixture, and the cutting angle of the cutting tool could be adjusted by adjusting the bolts on both sides of the cutting platform.



1. Microcomputer-controlled electronic universal material testing machine
2. Spherical cutting tool 3. Cutting platform 4. Broccoli

Figure 3 Schematic diagram of straw cutting force test bench

2.2 Mechanical characteristics test scheme design

In this experiment, diameter D , height H , stem diameter d and weight W of broccoli were measured as the physical characteristic parameters of broccoli. The measurement process is shown in Figure 4.

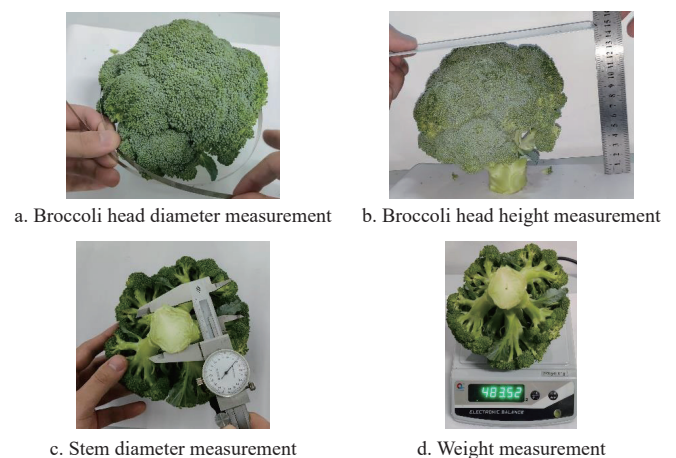


Figure 4 Measurement of physical characteristics of broccoli

During harvesting, the broccoli roots are rooted in the field, the position and posture remain unchanged, and the tools evenly distributed on both sides of the stem are used to cut the stem at the same time during harvesting. When the tool acts on the cutting point of the broccoli root, the position and posture of the broccoli change slightly and tend to be stable rapidly due to the relative force between the broccoli and the tool. Therefore, the process of broccoli stem cutting can be regarded as the cutting effect of the fixed tool at one end. During the experiment, the broccoli stalks were placed on two semi hollow cylindrical supports of the cutting test bench. There was 1 cm spacing between the two supports, and the flower heads were placed naturally. The spherical tool was fixed to the universal material testing machine through the fixture. The tool was lifted with the universal testing machine to cut the stalks at the support spacing to simulate the shear effect of the two tools on broccoli stalks in actual production. By adjusting the nut height of

the right support, changes in the right support height can be realized, thus changing the size of the cutting angle β . The cutting angle β is the angle between the centerline direction of the stem and the tool movement direction. In the actual harvesting process, the cutting angle is generally between 70° and 90° . These angles are considered on the basis of the blade angle of 30 degrees, which is generally related to the uprightness of plant growth and the neutrality of tool cutting. Therefore, in the experiment, cutting angles of 70° , 80° and 90° were selected to test the cutting force of broccoli stalk to compare the cutting force of the tool and the maximum cutting force of the stalk under different cutting angles. The maximum cutting force in the cutting process is obtained, which provides a reliable mechanical data for the follow-up study. The force sensor on the universal material testing machine and its own processing software can obtain the curve diagram and peak value of the relationship between load and displacement during the test. The load obtained by the sensor can be regarded as the cutting force of the tool. The peak value of the curve during the cutting process of the broccoli stem is used as the maximum cutting force F_r that the broccoli stem can withstand.

2.3 Mechanical characteristics test scheme design

2.3.1 Physical characteristics measurement results

In this experiment, 400 'Zheqing 161' broccoli were measured and counted. The main measurement contents were broccoli head diameter D , height H , stem diameter d and weight W . The four data were used as the physical characteristic parameters of broccoli. The diameter D of the mature broccoli 'Zheqing 161' is mainly distributed from 135-150 mm, with a total of 344, accounting for 86% of the total measured. The height of broccoli H is mainly distributed from 145-160 mm, a total of 351, accounting for 87.75% of the total measured. The stem diameter d is mainly distributed from 40-45 mm, a total of 267, accounting for 66.75% of the total measured. The broccoli weight W is mainly distributed from 350-500 g, a total of 400, accounting for 100% of the total measured.

2.3.2 Cutting force characteristic test results

In order to obtain the maximum cutting force of the stem, this experiment carried out a slow cutting test under the condition of keeping the water content of broccoli relatively sufficient. In this study, 20 broccolis were randomly selected from 400 broccolis for the stem cutting force test. To study the change in cutting force of the same broccoli at different cutting angles, the cutting force characteristics of 70° , 80° , and 90° were tested at 110 mm, 120 mm, and 130 mm below the flower head. Through the force sensor on the universal testing machine and its own processing software, the curve diagram and peak value of the relationship between load and displacement during the test can be obtained, as shown in Figure 5, which shows three cutting force curves with different cutting angles in the same set of tests. From the curve, it can be seen that the cutting force in the cutting process of broccoli roughly presents two ups and downs with the displacement, and the two ups and downs are generated in the cutting process of the upper and lower epidermis, respectively. Between the two ups and downs is the cutting process of the internal tissue, and the curve remains relatively stable compared to the beginning and end.

Twenty groups of cutting test results are listed in Table 1. When the cutting angle is 70° - 90° , the larger the cutting angle, the greater the cutting force required to cut the broccoli stem. When the cutting angle is 90° , the maximum cutting force is 90-120 N; when the cutting angle is 80° , the cutting force is 85-100 N; and when the cutting angle is 70° , the cutting force is 80-95 N. Comparing the diameter of broccoli stems in each group, the greater the diameter of

broccoli stems, the greater the cutting force needed. The diameter and cutting force of the seventh group were the largest, with a diameter of 48 mm and maximum cutting force of 113.2 N.

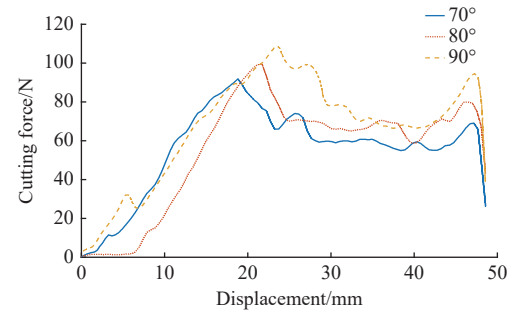


Figure 5 Cutting force-displacement curve

Table 1 Maximum cutting force F_r (N) of stem at different cutting angles

Test No.	Stem diameter/ mm	Cutting angle		
		90°	80°	70°
1	42	93.5	87.2	81.6
2	43	97.9	93.4	88.3
3	44	102.4	95.7	89.7
4	42	94.2	87.9	82.2
5	39	92.3	86.8	80.5
6	44	103.6	96.1	90.4
7	48	113.2	101.3	93.8
8	45	106.3	98.2	91.4
9	44	98.8	93.6	88.6
10	40	93.2	87.0	81.4
11	47	108.6	99.1	91.9
12	44	102.3	95.7	89.6
13	44	99.3	93.8	88.9
14	43	97.2	93.2	88.1
15	43	96.4	92.7	87.3
16	41	94.3	90.2	84.8
17	45	104.1	96.8	90.9
18	47	109.3	99.6	92.3
19	45	104.7	96.9	91.1
20	45	106.5	98.4	91.5

3 Design and optimization of end-effector

The agronomic requirements of broccoli harvesting are related to the design of the harvesting end-effector. Mature broccoli head plump, compact and dark green. The broccoli harvest needs to be carried out when the broccoli head is fully grown and has not flowered. Generally, the diameter of the head is 13-15 cm, and some stems need to be retained when harvesting the head. The length from the top of the head to the bottom of the stem needs to be 14 cm.

3.1 End-effector mechanism design

The broccoli harvesting end-effector is mainly responsible for stem cutting and flower heads recovery during the harvesting process. According to the growth environment of broccoli in the field and the agronomic requirements of harvesting, combined with the maximum load of the end of the harvesting manipulator is 5 kg and the quality of broccoli is generally 350-500 g, a broccoli harvesting end-effector needs to meet the following requirements:

1) During the harvesting process, the end-effector will not interfere with the broccoli, and the harvesting process will not cause

mechanical damage to the flower head.

2) The end-effector harvesting tool has good shear capacity and rigidity.

3) The overall weight of the end-effector is light and remains below 4 kg.

According to the broccoli field growth conditions, the end-effector needs to be harvested from above the broccoli head and should not be cut from the stem side. According to the end-effector harvesting method and cutting tool requirements, this paper uses a spherical cutting tool as the cutting tool for the harvesting end-effector. The spherical cutting tool has a good cutting ability during the shearing process and has good rigidity and strength^[23]. In the process of actual mechanical harvesting, the end-effector moves downward in the direction of the flower head, reaching a position 50 mm below the lower plane of the flower head, so that the blade of the spherical cutter removes part of the leaves wrapped in the flower head downward, so as to achieve the purpose of no blade blocking shear at the stem. Then the tool is raised to the highest horizontal plane of the spherical surface of the flower head, and the tool is closed to complete the cutting of the broccoli stem to achieve harvesting. According to the measurement of the physical characteristics of broccoli, the diameter of the mature broccoli head is 130-150 mm. Therefore, the inner diameter of the cutting tool on the left side of the end-effector is 156 mm, the outer diameter of the cutting tool on the right side of the end-effector is 156 mm, and the two cutting tools are both unilaterally cut. The thickness of the cutting tool is 4 mm, the installation distance of the two cutting tools is 40 mm, and the overcut of the cutting tool is 4 mm. When the tool is fully open, the width between the cutting edges is enough to wrap the flower head, and the stem rotates downward and cuts off until the tool is completely closed. To ensure that the end-effector has a lighter weight, this paper selects the crank-slider mechanism as the main structure of the end-effector. A structural diagram is shown in Figure 6. The end-effector takes the slider as the driving part and drives the connecting rod to rotate downward in the plane during the downward movement of the slider so that the crank rotates around the frame and drives the spherical cutting tool fixed at the crank to realize the closing of the left and right cutting tools to achieve the shearing effect.

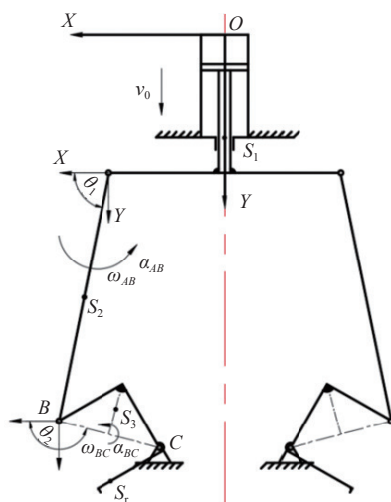


Figure 6 Structure diagram of end-effector

3.2 Kinematics analysis of end-effector

For the end-effector mechanism diagram shown in Figure 6, the kinematics analysis of the whole mechanism is carried out with the

slider as the prime mover to study the trajectory of the tool and the speed of the contact point during the tool movement. Because the mechanism is symmetrical and the difference between the left and right cutting tools is almost negligible, this paper only analyses the speed of the left side of the mechanism. In this study, the kinematics analysis of the mechanism is carried out using an analytical method. The Cartesian coordinate system shown in Figure 6 is established with the O point of the centerline as the origin. The vector angle takes the X -axis as the starting edge and the rod as the end edge, and the counter clockwise direction is defined as the positive direction of the angle. The mathematical model of the end-effector of broccoli harvesting is established. To facilitate the expression and review, the parameter symbols and meanings used in kinematics are listed in Table 2.

Table 2 Kinematic parameter symbols and description of end-effector

Sign	Explanation
$y_0(t)$	Displacement of the sliding-block
l_1/m	Distance between slider centre and hinge point A
l_2/m	Length of connecting rod AB
l_3/m	Length of crank BC
l_4/m	Distance between fixed hinge C and central axis
(x_B, y_B)	Moving hinge B point coordinates
$\theta_1/(\circ)$	Angle between rod AB and X -axis
$\theta_2/(\circ)$	Angle between rod CD and X -axis
r/m	Left cutting tool radius
r'/m	Distance between left tool centroid and centre of circle
(x_A, y_A)	Point A coordinate of moving hinge
(x_C, y_C)	Fixed hinge C point coordinates

3.2.1 Position analysis

According to the established coordinate system and rod length conditions, the A , B , and C three-point coordinates can be expressed as,

$$\begin{cases} x_A = l_1 \\ y_A = y_0(t) \end{cases} \quad (1)$$

$$\begin{cases} x_B = x_A + l_2 \cos \theta_1 \\ y_B = y_A + l_2 \sin \theta_1 \end{cases} \quad (2)$$

$$\begin{cases} x_C = x_B + l_3 \cos \theta_2 = l_1 + l_2 \cos \theta_1 + l_3 \cos \theta_2 \\ y_C = y_B + l_3 \sin \theta_2 = y_0(t) + l_2 \sin \theta_1 + l_3 \sin \theta_2 \end{cases} \quad (3)$$

According to the rod length condition $|\vec{AB}| = l_2$, $|\vec{BC}| = l_3$, the constraint equation of the end mechanism is

$$\begin{cases} (x_B - x_A)^2 + (y_B - y_A)^2 = l_2^2 \\ (x_B - x_C)^2 + (y_B - y_C)^2 = l_3^2 \end{cases} \quad (4)$$

Because the position of hinge points A and C is determined, the simultaneous Equations (1)-(4) can be obtained.

$$\begin{cases} \theta_1 = 2 \arctan \frac{a_1 - \sqrt{a_1^2 + b_1^2 - c_1^2}}{b_1 + c_1} \\ \theta_2 = 2 \arctan \frac{a_2 + \sqrt{a_2^2 + b_2^2 - c_2^2}}{b_2 + c_2} \\ x_B = l_1 + l_2 \cos \theta_1 \\ y_B = y_0(t) + l_2 \sin \theta_1 \end{cases} \quad (5)$$

where,

$$\begin{cases} a_1 = 2(y_C - y_A)l_2 \\ b_1 = 2(x_C - x_A)l_2 \\ c_1 = (x_C - x_A)^2 + (y_C - y_A)^2 + l_2^2 - l_3^2 \\ a_2 = 2(y_C - y_A)l_3 \\ b_2 = 2(x_C - x_A)l_3 \\ c_2 = (x_C - x_A)^2 + (y_C - y_A)^2 - l_2^2 + l_3^2 \end{cases} \quad (6)$$

3.2.2 Velocity analysis

The slider moves downward at a constant speed of v_0 . A derivation of Equation (2) and Equation (3) is calculated with respect to time. The angular velocity w_1 of the rod connecting rod AB , angular velocity w_2 of crank BC and velocity v_B of point B can be obtained by simultaneous equations as follows:

$$\begin{cases} \omega_{AB} = \frac{v_0 \sin \theta_2}{l_2 \sin(\theta_1 - \theta_2)} \\ \omega_{BC} = \frac{v_0 \sin \theta_1}{l_3 \sin(\theta_2 - \theta_1)} \\ v_{Bx} = -\omega_{AB} l_2 \sin \theta_1 \\ v_{By} = v_0 + \omega_{AB} l_2 \cos \theta_1 \end{cases} \quad (7)$$

3.2.3 Acceleration analysis

Because the slider moves downward at a constant speed of v_0 , the acceleration of the slider is 0. A derivation of Equation (7) was calculated with respect to time. The angular acceleration α_{AB} of connecting rod AB , angular acceleration α_{BC} of crank BC and acceleration a_B of point B are obtained as,

$$\begin{cases} \alpha_{AB} = -\frac{1}{l_2 \sin(\theta_1 - \theta_2)} (\omega_{AB}^2 l_2 \cos(\theta_1 - \theta_2) + \omega_{BC}^2 l_3) \\ \alpha_{BC} = -\frac{1}{l_3 \sin(\theta_2 - \theta_1)} (\omega_{BC}^2 l_3 \cos(\theta_2 - \theta_1) + \omega_{AB}^2 l_2) \\ a_{Bx} = -\alpha_{AB} l_2 \sin \theta_1 - \omega_{AB}^2 l_2 \cos \theta_1 \\ a_{By} = \alpha_{AB} l_2 \cos \theta_1 - \omega_{AB}^2 l_2 \sin \theta_1 \end{cases} \quad (8)$$

3.3 Dynamic analysis of end-effector

Because the cutting tool has speed during the movement, the cutting tool has an impact on the broccoli stem during the shearing process, which makes the smaller driving force cut off the broccoli stem. In this paper, the end mechanism is divided into two parts, as shown in Figure 7. Dynamic analysis of the crank and cutting tool parts based on the impulse distance theorem is carried out, and the remaining parts are analysed by the principle of dynamic virtual work to realize the dynamic analysis of the whole mechanism. In the dynamic analysis, some parameter symbols are shown in Figure 7. The parameter symbols and meanings used in kinematics are listed in Table 3.

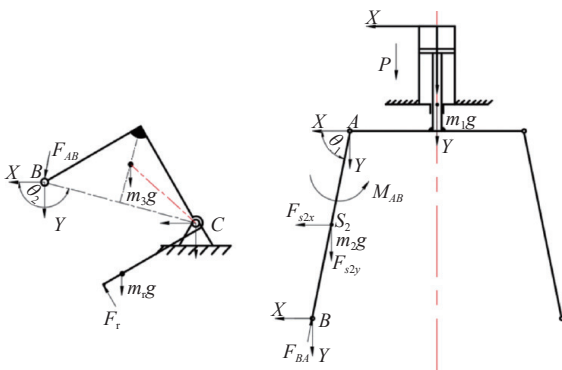


Figure 7 Dynamic analysis of the end-effector

Table 3 End-effector dynamics parameter symbols and instructions

Sign	Explanation
m_1 /kg	Slider mass
m_3 /kg	Crank BC mass
P /N	Driving force at slider
J_{s2} /kg·m ²	Moment of inertia at centroid of connecting rod AB
J_r /kg·m ²	Moment of inertia of cutting tool rotating around point C
(F_{AB}, F_{BA})	A pair of interaction forces at point B
m_2 /kg	Connecting rod AB mass
m_r /kg	Cutting tool mass
F_r /N	Cutting force
J_{BC} /kg·m ²	Moment of inertia of crank BC at C point
M_{AB} /N·m	Inertia moment of connecting rod AB
(F_{s2x}, F_{s2y})	Inertia force in x -, y -direction at centroid of connecting rod AB

Because the structure is symmetrical, only the left side of the mechanism is analysed. By analysing the crank-cutting tool mechanism and applying the impulse distance theorem, the following equation can be obtained:

$$(J_{BC} + J_r)(\omega'_B - \omega_B)/d_t = F_{AB} l_3 \sin(\theta_2 - \theta_1) + m_r g r' \cos \theta_{r1} - F_r r - \frac{\sqrt{5}}{4} m_3 g l_3 \cos(\theta_2 - 26.6^\circ) \quad (9)$$

where, d_t is the collision time between the cutting tool and the broccoli stem, generally 10^{-4} - 10^{-3} s, and θ_{r1} is the cutting angle of the tool, generally 70° - 90° .

Simplifying Equation (9), the acting force F_{AB} of connecting rod AB on the crank at point B is

$$F_{AB} = [(J_{BC} + J_r)(\omega'_B - \omega_B)/dt - m_r g r' \cos \theta_{r1} + F_r r + \frac{\sqrt{5}}{4} m_3 g l_3 \cos(\theta_2 - 26.6^\circ)] / [l_3 \sin(\theta_2 - \theta_1)] \quad (10)$$

Dynamic analysis of the structure of the slider connecting rod based on the virtual work principle is carried out. The dynamic problem is transformed into a static problem by the D'Alembert principle, and the virtual work principle is used to solve the problem. Now, the vertical downward virtual displacement δ is added at the driving force P , the direction of each active force (moment) is shown in Figure 6, and the virtual displacement at each active force (moment) is listed in Table 4. According to the above virtual displacement, the driving force P can be expressed as,

$$P = 2F_{BA} \sin \theta_1 + m_2 a_{s2x} \sin \theta_1 \sin \theta_2 / \sin(\theta_2 - \theta_1) - m_2 (g - a_{s2y}) (1 - \sin \theta_1 \cos \theta_2 / \sin(\theta_2 - \theta_1)) - 2J_{s2} \alpha_{AB} \sin \theta_2 / (l_2 \sin(\theta_2 - \theta_1)) - m_1 g \quad (11)$$

where,

$$\begin{cases} a_{s2x} = \frac{1}{2}(a_{Ax} + a_{Bx}) = \frac{1}{2}(-\alpha_{AB} l_2 \sin \theta_1 - \omega_{AB}^2 l_2 \cos \theta_1) \\ a_{s2y} = \frac{1}{2}(a_{Ay} + a_{By}) = \frac{1}{2}(\alpha_{AB} l_2 \cos \theta_1 - \omega_{AB}^2 l_2 \sin \theta_1) \end{cases}$$

Table 4 Virtual displacement of each driving force (moment)

Sign	Value	Direction
δ_{s1}	δ	Vertical
$\delta\theta$	$\delta \sin \theta_2 / (l_2 \sin(\theta_2 - \theta_1))$	Clockwise
δ_{s2x}	$\delta \sin \theta_1 \sin \theta_2 / 2 \sin(\theta_2 - \theta_1)$	Horizontal left
δ_{s2y}	$\delta(\sin(\theta_2 - \theta_1) - \sin \theta_1 \cos \theta_2) / 2 \sin(\theta_2 - \theta_1)$	Vertical
δ_{AB}	$\delta \sin \theta_1$	Down along AB

3.4 End-effector structure optimization

According to the results of the kinematics and dynamics analysis, this study optimized the structure of the end-effector. The optimization object is the length $l = [l_1, l_2, l_3]$ of the three-bar rod. The optimization goal is that the external driving force P of the end-effector is the lowest, and the driving force can be calculated by Equation (11). 1) Connecting rod and crank transmission angle greater than 45° during movement. 2) B point and A point in the X -axis direction distance greater than 10 mm. 3) Crank x -direction movement displacement difference within 10-40 mm. 4) The vertical distance between point C and point A at the initial position is 2.5 times greater than the slider stroke h . 5) Three rod length range is $l_1 \in [40, 80]$; $l_2 \in [100, 200]$; $l_3 \in [30, 70]$.

According to the actual cutting situation, the initial position $\theta_2 = 135^\circ$ of the mechanism is set in the optimization process, the end position $\theta_2 = 225^\circ$, cutting angle θ_{r1} of the tool is set to 80° , initial speed of the slider is 0.115 m/s, speed after collision is 0.1 m/s, maximum cutting force of the stem is 135 N (The maximum cutting force of 113.2 N is expanded by 1.2 times) and collision time is 10^{-3} s. Through dynamic analysis, the size of the external driving force P is related to the mass, length and angle of the rod. The mass of the rod is transformed by the linear density and the length of the rod so that the external driving force P is a function of only the length $l = [l_1, l_2, l_3]$ of the three rods. The mass conversion formula is

$$m = \lambda l \tag{12}$$

where, λ is the linear density of the rod, and the linear density of each rod is listed in Table 5.

Table 5 Linear density of each bar

Name	Slider l_1	Connecting rod l_2	Crank l_3
Linear density/kg·m ⁻¹	0.500	0.312	0.442

According to the optimization function and constraint conditions, the genetic algorithm function in the MATLAB library is used to optimize the rod length. The optimization convergence process is shown in Figure 8, and the optimization results are listed in Table 6.

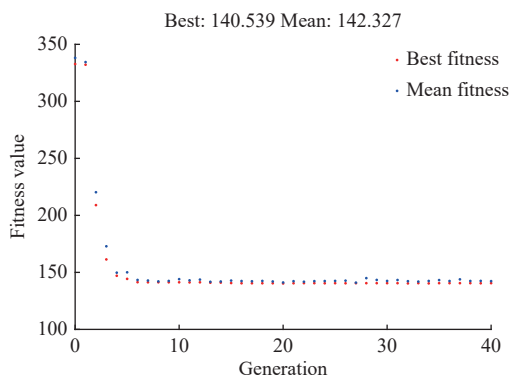


Figure 8 Optimization convergence process diagram

Table 6 Optimization results of rod length

Name	Slider l_1	Connecting rod l_2	Crank l_3
Length/mm	40.0014	120.4704	42.4401

According to the optimization results, the slider width l_1 is 40 mm, connecting rod length l_2 is 120 mm, and crank length l_3 is 42 mm. Substituting the rod length condition into Equation (11), the external driving force P is 140.54 N. The power source of the end-

effector needs good load capacity and fast speed. In this study, the cylinder is selected as the power source of the end-effector. The cylinder load rate is 50%, so the cylinder is required to provide power of at least 281.08 N. Therefore, the cylinder diameter is 32 mm.

4 Harvesting performance test of end-effector

4.1 Construction and experimental design of harvesting test platform

According to the results of structural optimization, the end-effector is processed and assembled. The physical prototype is shown in Figure 9. The harvesting test platform of the end-effector is built, and a harvesting performance test of the end-effector is carried out. The test platform is shown in Figure 10. The end-effector is fixed on the moving platform of the Delta manipulator, and the broccoli head is fixed on the fixed platform. The robot controller can realize the end-effector to feed the cutting tool from the top of the broccoli head, and the broccoli movement is placed in the harvesting basket after the tool is harvested. In the test, the cylinder pressure of the end-effector was 0.6 MPa, and broccoli of ‘ZheQing 161’ was selected as the test target. The cylinder moves at a pressure of 0.6 MPa, thus driving the tool to rotate through the connecting rod and cutting the broccoli.

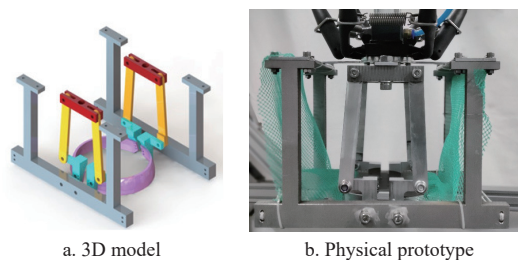
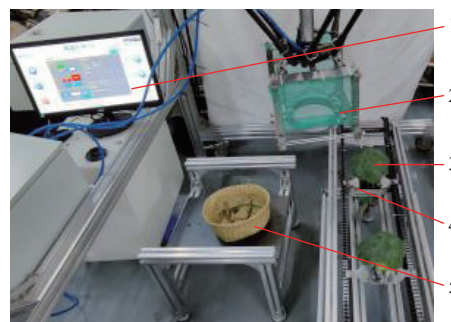


Figure 9 Broccoli harvesting end-effector



1. Robot control Panel 2. End-effector 3. Broccoli 4. Fixed platform 5. Storage basket

Figure 10 Broccoli harvesting test platform

The test process is as follows: the broccoli head is placed upwards, and the stem is fixed on the fastening device of the test platform. The end-effector moves slowly to the top of the broccoli head through the Delta manipulator and controls the cylinder to make the tool open and close. In this experiment, 30 groups of broccoli were randomly selected from 400 broccoli used in the test of Section 2.2, and the cutting effect of the test was recorded. The cutting performance of the end-effector was evaluated by observing the cutting surface of the broccoli stem.

4.2 Analysis of harvest test results

In the process of broccoli harvesting, the broccoli head is not easily damaged, so the success rate of stem cutting is particularly important for the performance of the harvesting end-effector. In this

study, the harvesting performance of the end-effector was evaluated by the success rate of whole cutting and the cutting condition of the stalk section. The calculation formula of the cutting success rate is shown in Equation (13), and the cutting effect of the end-effector on the broccoli stem is divided into three types: smooth section, uneven section and no section. The specific cutting end effect diagram is shown in Figures 11a-11c, and broccoli with a section is defined as successful cutting.

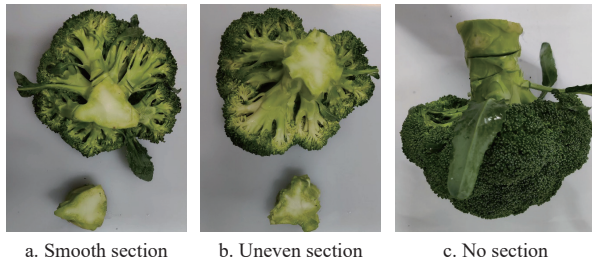


Figure 11 Cutting section effect of broccoli stem

$$P_g = \frac{T_g}{N_g} \times 100\% \quad (13)$$

where, P_g is the stem cutting success rate, %; T_g is the number of broccoli cut successfully; N_g is the total number of broccoli cut.

In this study, 30 groups of broccoli were harvested, and cutting sections of broccoli stems were measured and observed. The experimental data are listed in Table 7. In the experiment, the

Table 7 Statistics of broccoli stem cutting data

Number	Cut-off status (Y/N)	Stem diameter/mm	Sectional effect
1	Y	42	I
2	Y	39	I
3	Y	40	I
4	Y	39	I
5	Y	40	I
6	Y	38	I
7	Y	41	I
8	N	47	III
9	Y	42	I
10	Y	40	I
11	Y	41	I
12	Y	45	II
13	Y	44	I
14	Y	38	I
15	Y	45	I
16	Y	41	I
17	Y	43	I
18	Y	42	I
19	Y	41	I
20	N	48	III
21	Y	45	II
22	Y	39	I
23	Y	41	I
24	Y	44	I
25	Y	46	II
26	Y	42	I
27	Y	41	I
28	Y	40	I
29	Y	37	I
30	Y	36	I

Note: I : section is smooth, II : section is uneven, and III: section is not cut and no section is produced.

number of cutting effects of the three stems was 25, 3, and 2, respectively. The cutting success rate of the end-effector for broccoli stems was 93.3%, and most of them were completely cut off, with smooth sections accounting for 83.3% of the total. Some sections had an uneven feeling, accounting for 10.0% of the total. This was because the broccoli stem was not completely cut off by the cutting tool but was ripped off during the upward movement of the manipulator. The remaining portion, which accounted for 6.7% of the total, did not produce a cut because the stem was thick and uncut by the cutter.

According to the test results, the shorter the diameter of the broccoli stem, the easier it is to be completely cut off by the cutting tool during the cutting process. Smooth sections of broccoli stem diameter are below 45 mm, not completely cut off the broccoli stem diameter is generally 45-46 mm, and not cut off the two groups of broccoli stem diameter were 47 mm and 48 mm. During the cutting process, because the stem is too thick, the outer epidermis of the stem has strong toughness and deep lignification, and the cutting tool cannot break through the outer epidermis of the stem, resulting in cutting failure.

5 Conclusions

1) The physical and mechanical characteristics of broccoli ‘ZheQing 161’ were tested. The diameter of the broccoli head was 135-150 mm, height was 145-160 mm, weight was 350-500 g, diameter of the stem was 40-45 mm, and maximum cutting force of the stem was 80-115 N.

2) A broccoli harvesting end-effector was designed, and its kinematics, dynamics analysis and mechanism optimization were carried out. The slider width was 40 mm, connecting rod length was 120 mm, and crank length was 42 mm. According to the general harvesting condition, the required external driving force was calculated to be 140.54 N, and a 32 mm cylinder with a load rate of 50% was selected as the power source.

3) A harvesting test of the end-effector was completed. The overall harvesting success rate of the end-effector was 93.3%, and the stem section smoothness rate was 83.3%, which verified the harvesting performance of the broccoli end-effector.

Acknowledgements

The authors acknowledge that this work was financially supported by the Key Research Projects of Zhejiang Province (Grant No. 2022C02042; 2022C02002), the National Natural Science Foundation of China (Grant No.32071909), the Shanghai Science and Technology Agricultural Development Project 2021 (No.4-1), and the General Project of Agriculture and Social Development in Hangzhou (Grant No.202203B08; 20201203B92).

[References]

- [1] National Bureau of Statistics. China Statistical Yearbook: Beijing, China Statistics Press, 2020. (in Chinese)
- [2] Hu M H, Li J N. Analysis of the development status and constraints of vegetable production mechanization. Modern horticulture, 2017; 20: 18. (in Chinese)
- [3] Li H B, SHI Y. Review on orchard harvesting robots. China Agricultural Informatics, 2019; 31(6): 1-9. (in Chinese)
- [4] Liu J Z. Research progress analysis of robotic harvesting technologies in greenhouse. Transactions of the CSAM, 2017; 48(12): 1-17. (in Chinese).
- [5] Hayashi S, Shigematsu K, Yamamoto S, Kobayashi K, Kohno Y, Kamata J. Evaluation of a strawberry-harvesting robot in a field test. Biosystems Engineering, 2010; 105(2): 160-171.
- [6] Morar C A, Doroftei I A, Doroftei I, Hagan M. Robotic applications on

- agricultural industry. a review. *IOP Conference Series Materials Science and Engineering*, 2020; 997(1): 012081.
- [7] Oliveira L F P, Moreira A P, Silva M F. Advances in agriculture robotics: a state-of-the-art review and challenges ahead. *Robotics*, 2021; 10(2): 52.
- [8] Shamshiri R R, Weltzien C, Hameed I A, Yule I J, Grift T E, Balasundram S K, et al. Research and development in agricultural robotics: A perspective of digital farming. *Int J Agric & Biol Eng*, 2018; 11(4): 1–14.
- [9] Wang Z H, Xun Y, Wang Y K, Yang Q H. Review of smart robots for fruit and vegetable picking in agriculture. *Int J Agric & Biol Eng*, 2022; 15(1): 33–54.
- [10] Oliveira F, Tinoco V, S. Magalhaes S, Santos F N and M. F. Silva M F. End-effectors for harvesting manipulators-state of the art review. 2022 IEEE International Conference on Autonomous Robot Systems and Competitions (ICARSC), 2022; 98–103.
- [11] Arikapudi R, Vougioukas S G. Robotic tree-fruit harvesting with telescoping arms: a study of linear fruit reachability under geometric constraints. *IEEE Access*, 2021; 9: 17114–17126.
- [12] Li M T, He L, Yue D D, Wang B B, Li J L. Fracture mechanism and separation conditions of pineapple fruit-stem and calibration of physical characteristic parameters. *Int J Agric & Biol Eng*, 2023; 16(5): 248–259.
- [13] Lu R, Dickinson N, Lammers K, Zhang K X, Chu P Y, Li Z J. Design and evaluation of end effectors for a vacuum-based robotic apple harvester. *Journal of the ASABE*, 2022; 65(5): 963–974.
- [14] Li B L, Ji C Y, Gu B X, Xu W Y, Dong M. Kinematics analysis and experiment of apple harvesting robot manipulator with multiple end-effectors. *Transactions of the CSAM*, 2016; 47(12): 14–21. (in Chinese)
- [15] Wang Y, Xu H B, Zhang M, Ma J T, Liu B, He Y. Design and experiment of bite-model end-effector for citrus harvesting by simulating with mouth of snake. *Transactions of the CSAM*, 2018; 49(10): 54–64. (in Chinese)
- [16] Wei B, He J Y, Shi Y, Jiang L G, Zhang X Y, Ma Y. Design and experiment of underactuated end-effector for citrus picking. *Transactions of the CSAM*, 2021; 52(10): 120–128. (in Chinese)
- [17] Guo T Z, Zheng Y F, Bo W X, Liu J, Pi J, Chen W, et al. Research on the bionic flexible end-effector based on tomato harvesting. *Journal of Sensors*, 2022; 2022: 2564952.
- [18] Liu J Z, Peng Y, Faheem M. Experimental and theoretical analysis of fruit plucking patterns for robotic tomato harvesting. *Computers and Electronics in Agriculture*, 2020; 173: 105330.
- [19] Qian S M, Yang Q H, Wang Z H, Bao G J, Zhang L B. Research on holding characteristics of cucumber and end-effector of cucumber picking. *Transactions of the CASE*, 2010; 26(7): 107–112. (in Chinese)
- [20] Zhao Y W, Geng D X, Liu X M, Sun G D. Kinematics analysis and experiment on pneumatic flexible fruit and vegetable picking manipulator. *Transactions of the CSAM*, 2019; 50(8): 31–42. (in Chinese)
- [21] Bac C W, Roorda T, Reshef R, Berman S, Hemming J, Henten E J. Analysis of a motion planning problem for sweet-pepper harvesting in a dense obstacle environment. *Biosystems Engineering*, 2016; 146: 85–97.
- [22] Barth R, Hemming J, Henten E J. Design of an eye-in-hand sensing and servo control framework for harvesting robotics in dense vegetation. *Biosystems Engineering*, 2016; 146: 71–84.
- [23] Chen J N, Chen L Q, Yu C N, Cai S L, Xia X D. Study on blade parameter optimization analysis of broccoli cuts based on minimum slice stress. *Transactions of the CASE*, 2018; 34(23): 42–48. (in Chinese)